Stability Improvement of Microgrids Using a Novel Reduced UPFC Structure via Nonlinear Optimal Control

Hossein Saberi, Shahab Mehraeen, and Boyu Wang
Division of Electrical and Computer engineering
Louisiana State University
Baton Rouge, LA, USA
hsaber1@lsu.edu, smehraeen@lsu.edu, bwang14@lsu.edu

***Abstract*— A reduced Unified Power Flow Controller (UPFC) structure is proposed to enhance transient stability of small-scale micro grids. The micro grid utilizes Photovoltaic (PV) unit as the Distributed Generation (DG) unit that is connected to the grid through dc-dc buck converter and inverter. The dc-dc converter provides a constant dc voltage at the output that is connected to the inverter. The inverter generates the proper ac voltage according to the system requirements to feed the gird. The reduced UPFC model exploits dc link of the DG unit to generate appropriate series voltage and inject it to the power line to enhance transient stability. It employs the nonlinear discrete-time Hamilton-Jacobi-Bellman (HJB) optimal control to ensure that the stability of the system is realized through minimum cost for the system. A Neural Network (NN) is used to approximate the cost function based on the weighted residual method. In order to verify efficiency of the proposed model and control scheme, the DG unit and proposed UPFC structure are tested in simulations and experiments. The results shows effective performance of the proposed approach in damping oscillations in the system.**

Keywords—Distributed Generation, FACTS devices, nonlinear control, transient stability

I. INTRODUCTION

Application of Flexible AC Transmission System (FACTS) devices are increasing for power quality and stability improvement in the power systems. One of the most attractive devices is Unified Power Flow Controller (UPFC) that is used in transmission systems for power flow control and transient stability improvement. Also, it can be utilized in distribution systems and micro grids to improve transient stability in addition to power flow control. In small-scale power systems and micro grids with low stored energy level, transient stability of the system is of utmost importance while various disturbances threaten stability of the system.

The UPFC consists of two main parts: shunt and series branches that are coupled together through a dc link. The shunt branch control voltage at the shunt bus through absorbing or injecting required reactive power. It also absorb the necessary active power from the grid to provide a constant voltage at the dc link. Although some dynamic variation are observable at the dc link voltage, it should be kept constant in steady state to achieve desired performance of the UPFC [1]. The series branch inject a series voltage to the power lines that is controlled for different purposes such as direct voltage injection, phase angle shifter and line impedance emulator, and automatic power flow control. The automatic power flow control can also be employed for oscillation damping and stability improvement. Thus, the injected series voltage can be controlled such that system stability is enhanced.

Different controllers can be used to determine the required series voltage based on states of the systems. Previously, linear approaches has been utilized to control the power systems [2-7]. In those methods, the system is linearized around an operating point so that linear methods are applicable providing the system remains in a small neighborhood around the operating point that is not always a correct assumption. However, since the power systems are inherently nonlinear, nonlinear approaches are more appropriate. In addition, employing an optimal nonlinear control method minimizes the cost that is defined as a function of states and control variables [8-11]. The optimal nonlinear control method can be derived by solving the Hamilton–Jacobi–Bellman (HJB) equation.

Recently, renewable energy resources, especially Photovoltaic (PV) units, have attracted more attention as environment-friendly and abundant resource of energy. In order to integrate solar energy into the grid several methods and technologies are presented such as microinverters [12-13]. The main goal has been extracting maximum power out of the PV sources and inject it to the grid properly. Those methods are appropriate when the share of energy that comes from renewable energy resources is negligible. However, in a grid that the renewable energy resources generate a considerable share of energy Distributed Generation (DG) units should also contribute in power system control and stability [14].

In this paper, a small-scale micro grid that consists of DG units as the sources of energy is studied. The DG units are Photovoltaic (PV) units that are connected to the grid via dc-dc buck converters and inverters. The DG units are modeled and controlled to operate similar to a synchronous generator

Research is supported in part by NSF CAREER ECCS#1151141.

classical model in the power system. In order to improve the transient stability of the system, a novel reduced UPFC structure is proposed that decreases the implementation cost of the UPFC considerably. Also, an optimized mechanism is utilized for the UPFC control to stabilize the power system by imposing the minimum cost. The minimized cost function results in lower stress on power electronics devices that increase their lifetime.

II. MODELING AND CONTROL OF THE SYSTEM

The DG unit utilizes a PV source as primary source of energy. A dc-dc buck converter connects the PV unit to the inverter through a dc link capacitor. The dc-dc converter provides a constant voltage at the dc link regardless of voltage variation at the PV's output terminals. The regulated dc voltage is also used by the reduced UPFC to generate the required series voltage and inject it to the grid's power lines to enhance system stability. In this section first the DG unit modeling and control is presented and then, modeling and control of the UPFC is developed.

A. DG Unit Modeling and Control

The DG unit is modeled and controlled such that mimic behavior of a synchronous generator. Dynamic equations for the power at the dc link can be written as

$$CV_C\dot{V}_C = P_{in} - P_o \tag{1}$$

where P_{in} is the power that is injected to the capacitor from the dc-dc buck converter, P_o is the delivered power to the inverter, and V_c is the capacitor voltage. On the other hand, the inverter's delivered power to the grid will be

$$\overline{P}_e = BV_sV_1\sin(\varphi-\theta) \tag{2}$$

where B is the admittance that connect the inverter to the grid bus, V_s and φ are the voltage magnitude and phase angle at the inverter's output terminals, and V_1 and θ are the grid bus's voltage magnitude and phase angle. Neglecting the inverter's losses results in $\overline{P}_e = P_o$

In (2), the angle φ behaves similar to the stator angle δ in the synchronous generator and the inverters output power can be adjusted through changing this variable. A new variable λ is introduced to control φ in the inverter as

$$\lambda = \dot{\varphi} \tag{3}$$

λ is similar to the rotor speed (ω) in the synchronous generator. The rotor speed define its stored kinetic energy as

$$\dot{\omega} = (1/M)(P_m - P_{elec}) \tag{4}$$

where M is the moment of inertia, P_m is the input mechanical power and P_{elec} is the output electrical power. In order to relate the new variable λ to the stored energy in the dc link capacitor, it can be defined as

$$\dot{\lambda} = (1/C)(P_{in} - P_o) \tag{5}$$

Equations (3) and (5) resemble the equations of a synchronous generator classical model. In order to mimic the droop mechanism in synchronous generators, any deviation from the steady state value of λ will result in some change in the dc-dc converter's duty factor, D. This adjustment subsequently changes the operating point of the PV unit which alters its output power. Thus, any variation in λ follows by some change in the injected power which comes from the dc side that pull back the λ to its steady state value.

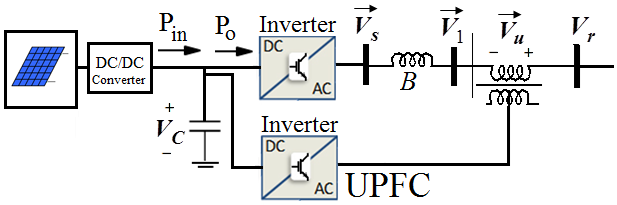

Fig. 1. System composed of DG and UPFC

B. Modeling and Control of the System in Presence of the UPFC

The vector diagram of the system shown in Fig. 1 is depicted in Fig. 2. The series voltage of the UPFC is composed of two components V_{up} and V_{uq}. The voltage components are considered to be proportional to the voltage at the point of connection of the UPFC. Consequently,

$$V_{uq} = V_r\beta(t),\ V_{up} = V_r\gamma(t) \tag{6}$$

where β(t) and γ(t) are two control variables. When the UPFC is taken into account, the electrical power in (2) can be written as

$$P_e = V_sV_1B\sin(\varphi-\theta) = V_sV_1B(\sin\varphi\cos\theta - \cos\varphi\sin\theta) \tag{7}$$

Based on the diagram in Fig .2,

$$\cos\theta = \frac{V_{uq}+V_r}{V_1} = \frac{(1+\beta)V_r}{V_1}$$

$$\sin\theta = \frac{V_{up}}{V_1} = \frac{(\alpha)V_r}{V_1} \tag{8}$$

Substituting (8) and (9) into (7), dynamics of the variable λ can be expressed as

$$\begin{aligned} C\dot{\lambda} &= P_{in} - V_sV_rB\sin(\varphi) - D\lambda \\ &+ V_sV_rB\cos(\varphi)\alpha(t) - V_sV_rB\sin(\varphi)\beta(t) \end{aligned} \tag{9}$$

According to the (3) and (10) the space state equations of the system will be written in the form of $\dot{x} = f(x) + g(x)u(t)$ as follows

$$\begin{bmatrix}\dot{\varphi}\\ \dot{\lambda}\end{bmatrix} = \begin{bmatrix}\lambda\\ \frac{1}{C}(P_{in} - V_sV_rB\sin(\varphi) - D\lambda)\end{bmatrix} + \begin{bmatrix}0 & 0\\ \frac{1}{C}V_sV_rB\cos(\varphi) & -\frac{1}{C}V_sV_rB\sin(\varphi)\end{bmatrix}\begin{bmatrix}\gamma\\ \beta\end{bmatrix} \tag{10}$$

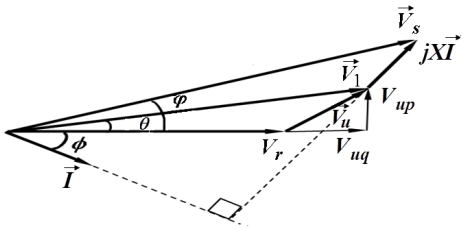

Fig. 2. Vector diagram of DG and UPFC

By assuming the time step T, the system dynamic equations can be approximated in discrete-time by

$$\begin{bmatrix}\varphi(k+1)\\ \lambda(k+1)\end{bmatrix}=\begin{bmatrix}\lambda T+\varphi(k)\\ \frac{T}{C}(P_{in}-V_sV_rB\sin(\varphi(k))-D\lambda(k))+\lambda(k)\end{bmatrix}+ \quad (11)$$
$$\begin{bmatrix}0 & 0\\ \frac{T}{C}V_sV_rB\cos(\varphi) & -\frac{T}{C}V_sV_rB\sin(\varphi)\end{bmatrix}\begin{bmatrix}\gamma\\ \beta\end{bmatrix}$$

Next, an optimal nonlinear control approach is applied to create the inputs β and γ according to the system states γ, λ.

III. NONLINEAR OPTIMAL CONTROLLER DESIGN

A. Control Objective

Consider the affine nonlinear state feedback discrete-time system as

$$x_{k+1}=f_k+g_ku_k \quad (12)$$

where $x_k=x(k)\in\Re^n$ is the state vector at step k, $f_k=f(x_k)$, $f(.)\in\Re^n$, $g_k=g(x_k)$, are input gain functions which are smooth and defined in a neighborhood of the origin, $u_k=u(x_k)\in\Re^m$, is the control input. Assume that $f_k+g_ku_k$ is Lipschitz continuous and there exists a control policy that can asymptotically stabilized the system. Then, the task is converted to find a control input u_k that minimizes the generalized quadratic discrete time cost function

$$V_k=\sum_{j=k}^{\infty}(Q(x_j)+u_j^TRu_j)=Q(x_k)+u_k^TRu_k+V_{k+1} \quad (13)$$

where Q and R are positive definite matrices. Meanwhile, the control policy u_k needs not only stabilizes the system, but guarantees the cost function V_k is finite, which means u_k is admissible.

Definition 1. (Admissible Control): a piecewise continuous state feedback control $u(x(k))$ is said to be an admissible control if it can not only stabilize the system but also guarantee the cost function to be finite, which means $J_k=J(x(0),u_k)<\infty$.

Note that, admissible input can make sure the system convergence, however, not all converged control input are admissible [8].

Thus, define the Hamiltonian function as

$$H(x_k,u_k)=V(f_k+g_ku_k)-V(x_k)+Q(x_k)+u_k^TRu_k \quad (14)$$

According to the Bellman optimality principle [9] the goal is to minimize the Hamiltonian function, and when it goes to zero, we will have discrete-time HJB equation [8]

$$V(f_k+g_ku_k^*)-V(x_k)+Q(x_k)+u_k^{*T}Ru_k^*=0 \quad (15)$$

where the optimal control policy u_k^* is the solution of (13).

By utilizing the stationary conditions, the optimal control policy u_k^* can be realized from $\partial H(x_k,u_k,w_k)/\partial u_k=0$ as

$$u_k^*=-1/2\,R^{-1}g_k^T\,\partial V_{k+1}^*/\partial x_{k+1} \quad (16)$$

Next, by substituting (16) into (15), the HJB equation becomes

$$V_{k+1}^*-V_k^*+Q(x_k)+1/4\left(\partial V_{k+1}^*/\partial x_{k+1}\right)^T\times \left(-g_kR^{-1}g(x_k)^T\right)\partial V_{k+1}^*/\partial x_{k+1}=0 \quad (17)$$

Due to the nature of partial derivatives $\partial V_{k+1}^*/\partial x_{k+1}$ and nonlinearly of the equation, it is still a challenging task to solve (17). Therefore, applying Tylor series expansion is one way to overcome the obstacle. The difference of two adjacent cost function ΔV_k can be expanded by remaining the first and second order terms in the Taylor Series and ignoring higher order terms. In other words, higher order terms can be treated as small disturbances around the operating points. Thus, we obtain

$$\Delta V_k=V_{k+1}-V_k\approx\nabla V_k^T(x_{k+1}-x_k)+\frac{1}{2}(x_{k+1}-x_k)^T\nabla^2V_k(x_{k+1}-x_k) \quad (18)$$

where ∇V_k and ∇^2V_k are the gradient vector and Hessian matrix, respectively. Then, we obtain generalized HJB equation (19), by substituting (18) into (14).

$$Q(x_k)+u_k^TRu_k+\nabla V_k(f_k+g_ku_k-x_k)+ \frac{1}{2}(f_k+g_ku_k-x_k)^T\nabla^2V_k(f_k+g_ku_k-x_k)=0. \quad (19)$$

With the new GHJB equation, another Hamiltonian function needs to be defined as Definition 2.

Definition 2. (Pre-Hamiltonian Function): A suitable pre-Hamiltonian function for the affine nonlinear discrete-time system (12) is defined as

$$H(x_k,V_k,u_k)=\nabla V_k(f_k+g_ku_k-x_k)+\frac{1}{2}(f_k+g_ku_k-x_k)^T\nabla^2V_k(f_k+g_ku_k-x_k)+Q(x_k)+u_k^TRu_k. \quad (20)$$

The new optimal control policy u_k^* can be derived as

$$u_k^*=-\left[g_k^T\nabla^2V_kg_k+2R\right]^{-1}g_k^T\left[\nabla V_k^T+\nabla^2V_k(f_k+h_kw_k^*-x_k)\right] \quad (21)$$

Now, the optimal control policy contains only the current step states x_k and get rid of x_{k+1} compare to policy (16). However, the solution of GHJB is still challenging to solve

and the value function remains unknown. A successive approximation methodology is utilized by updating the approximation of GHJB and controller every iteration until it reaches to the optimal policy. In each iteration, a critic NN is applied to approximate the value function to adjust the weights vector.

B. Value Function Approximation using Neural Network

As previously discussed, the successive approximation method can be used to find the optimal control policy with modified linear GHJB (20). However, recursively solving GHJB and updating controller is impossible without knowing V_k . Before the iterative based method is implemented, V_k is approximated by NN. The NN is well known for smooth function approximation and been widely used in previous research. Thus, it is an appropriate approach for our discrete-time problem.

A nonlinear function can be approximated by a NN as

$$V_L(x) = \sum_{l=1}^{L} \omega_l \sigma_l(x) = W_L^T \bar{\sigma}_L(x) \tag{22}$$

where L is the number of neurons in the hidden layer, ω_l, are NN weights and the activation function vector $\sigma_l(x)$ .Then the activation function and weights are vectored as $\bar{\sigma}_L = [\sigma_1 \quad \cdots \quad \sigma_L]^T$ and $W_L = [\omega_1 \quad \cdots \quad \omega_L]^T$. The residual error will be minimized by adjusting the weights in each iteration and be evaluated by least squares method. The solution will guarantee the lowest weights residual error.

A residual error is set as

$$GHJB\left(V_L^{(i)} = \sum_{l=1}^{L} \omega_l \sigma_l(x), u^{(i)}\right) = e_L(x) \tag{23}$$

where V_L denotes the approximation of the cost function. The weights ω_l are obtained by $\frac{\partial e_L(x)}{\partial W_L} = 0 \quad \forall \; x \in \Omega$,which means the error remains unchanged with respect to current weights. i.e.

$$\left\langle \frac{\partial e_L(x)}{\partial W_L}, e_L(x) \right\rangle = 0 \tag{24}$$

Substituting (18) and (22) into (24) yields

$$\left\langle \nabla\bar{\sigma}_L \Delta x + \frac{1}{2}\Delta x^T \nabla^2 \bar{\sigma}_L \Delta x, \nabla\bar{\sigma}_L \Delta x + \frac{1}{2}\Delta x^T \nabla^2 \bar{\sigma}_L \Delta x \right\rangle W_L + \left\langle Q(x) + u^T R u, \nabla\bar{\sigma}_L \Delta x + \frac{1}{2}\Delta x^T \nabla^2 \bar{\sigma}_L \Delta x \right\rangle = 0 \tag{25}$$

where the terms $\nabla\bar{\sigma}_L$ and $\nabla^2\bar{\sigma}_L$ are gradient vector and Hessian matrix of $\bar{\sigma}_L(x)$ with respect to x, respectively, and $\Delta x = f(x) + g(x)u(x) - x$.

By defining $\left\{\nabla\sigma_j^T \Delta x + \frac{1}{2}\Delta x^T \nabla^2 \sigma_j \Delta x\right\}_1^L$ as $\bar{\theta}$, the current weight vector can be written as

$$W_L = -\left\langle \bar{\theta}, \bar{\theta} \right\rangle^{-1} \left\langle Q(x) + u^T R u, \bar{\theta} \right\rangle \tag{26}$$

In [8], the term $\left\langle \bar{\theta}, \bar{\theta} \right\rangle$ is shown to be full and therefore, it can be inverted, which means a unique solution W_L exists. In Hilbert space, inner product is defined as

$$\left\langle a(x), b(x) \right\rangle = \int_{\Omega} a(x)b(x)dx \approx \sum_{i=1}^{N} a(x)b(x)\delta x \tag{27}$$

Calculating the integration in (27) is computationally costly. However, by utilizing the Riemann definition of integration, it is reasonable to approximate the integration in a acceptable degree. This leads to a nearly optimal solution algorithm.

A mesh is generated on Ω , where the mesh size is δx , that is around the operation points ,(26) can be simplified as

$$W_L = -\left(X^T X\right)^{-1} XY \tag{28}$$

where X and Y are in vector form as

$$X = \left[\left(\nabla\bar{\sigma}_L \Delta x + \Delta x^T \nabla^2 \bar{\sigma}_L \Delta x/2\right)_{x=x_1} \quad \cdots \quad \left(\nabla\bar{\sigma}_L \Delta x + \Delta x^T \nabla^2 \bar{\sigma}_L \Delta x/2\right)_{x=x_p}\right]^T \tag{29}$$

$$Y = \begin{bmatrix} \left(Q(x) + u^{(i)^T} R u^{(i)}\right)_{x=x_1} \\ \vdots \\ \left(Q(x) + u^{(i)^T} R u^{(i)}\right)_{x=x_p} \end{bmatrix} \tag{30}$$

where p in x_p denotes the number of points of the mesh. This number increases as the mesh size is reduced. Note that activation function should be continuous and linearly independent. The mesh must generate more points compare to the order of the approximation L to guarantee the convergence. These conditions make sure $(X^T X)$ is full rank [10].

C. Successive Approximation of the Approximate HJB Equation

The successive approximation procedure starts with a selected initial admissible control policy $u_k^{(0)}$, iteratively updates the control input $u_k^{(i)}$ in a loop with index i. Then, the pre-Hamiltonian equation (20) is solved for $V_k^{(i)}$ as

$$\nabla V_k^{(i)}(f_k + g_k u_k^{(i)} - x_k) + \frac{1}{2}(f_k + g_k u_k^{(i)} - x_k)^T \times \nabla^2 V_k^{(i,j)}(f_k + g_k u_k^{(i)} - x_k) + Q(x_k) + u_k^{(i)^T} R u_k^{(i)} = 0. \tag{31}$$

Next, $u_k^{(i)}$ is updated as

$$u_k^{(i+1)} = -[g_k^T(\nabla^2 V_k^{(i)})g_k + 2R]^{-1} g_k^T \times [\nabla V_k^{(i)^T} + \nabla^2 V_k^{(i)}(f_k - x_k)] \tag{32}$$

Then, next step value function is calculated by solving (31) for $V_k^{(i)}$. The iterations proceed until it converges i.e. $V_k^{(i)} = V_k^{(i+1)} = V_k^{(\infty)}$.

The convergence is proved using the following theorem.

Theorem 1. With $u_k^{(i)}$ be an admissible control for system (10) on the compact set Ω . Then, the nonlinear system

$x_{k+1} = f(x_k) + g(x_k)u_k^{(i+1)}$ satisfies $V_k^{(i)} \geq V_k^{(i+1)} \geq V_k^{(*)}$ and $\lim_{i\to\infty} V_k^{(i)} = V_k^{(*)}$ where $V_k^{(*)}$ solves the approximate GHJB equation (13). Also, if $V_k^{(i)} = V_k^{(i+1)}$, then $V_k^{(i)} = V_k^*$.

An advantage of successive approximation is improved control policy according to the last step value function approximation that can guarantee the next step control policy to be admissible controller. Also, GHJB avoids the nonlinearity of the HJB that contains nonlinear partial differential equations. Now, using the successive approximation method and the approximation of GHJB by NN, the algorithm is presented as the following 5 steps:

1) Define a NN as $V = \sum_{l=1}^{L} \omega_l \sigma_l(x)$ to approximate smooth function of *V(x)*. Choose an admissible state feedback control policy $u^{(0)}$.

2) For *ith* step, find $V^{(i)}$ associated with $u^{(i)}$ to assure the approximate HJB by utilizing least square manner to find the NN weights W^i;

3) Update the control as

$$u_k^{(i+1)} = -\left[g_k^T\left(\nabla^2 V_k^{(i)}\right)g_k + 2R\right]^{-1} g_k^T \cdot \left[\nabla V_k^{(i)} + \left(\nabla^2 V_k^{(i)}\right)(f_k - x_k)\right] \quad (32)$$

4) Find $V^{(i+1)}$ associated with $u^{(i+1)}$ to assure the approximate HJB by utilizing least square method to find the NN weights W^{i+1};

5) If $V^{(i)}(0) - V^{(i+1)}(0) \leq \varepsilon$, where ε is the stopping criteria as a small enough constant, then $V^* = V^{(i)}$ and stop. Otherwise, $i=i+1$, go to step2.

Once V^* is obtained, the optimal state feedback control policy will be

$$u_k^* = -\left[g_k^T\left(\nabla^2 V_k^*\right)g_k + 2R\right]^{-1} g_k^T \cdot \left[\nabla V_k^* + \left(\nabla^2 V_k^*\right)(f_k - x_k)\right] \quad (33)$$

IV. Test Results

The simulations are carried out in Matlab/Simulink environment. The DG unit that is equipped with the UPFC is connected to a micro grid as shown in Fig. 3.

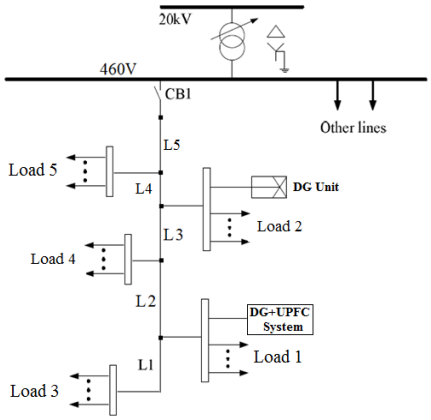

Fig. 3 Low voltage microgrid with DG and UPFC

TABLE I. System Parameters

PV Parameters	Value	DG Parameters	Value	Grid Parameters	Value
V_{oc}	39.5V	C_{in}	8.2mF	Line Resistance	0.5Ω
V_{mpp}	34V	L	2.5mH	Line Inductance	20mH
P_{mpp}	280W	C_{out}	8.2mF	V_{base}	200V
I_{sc}	9.7A	L_f	3mH	S_{base}	2kW
		C_f	47μF		

In addition, the microgrid includes another PV-based DG unit, five loads at five buses of the system, and transmission lines that are modeled as series RL branches. All the system definitions are given in Table I. As a case study, a fault happens on bus 1 where the DG with UPFC unit is connected. The fault occurred at t=3s and is removed after 0.2s. The presented optimal nonlinear controller regulate the injected series voltage of the UPFC in order to damp the after fault oscillations of the system. The offline training is performed in order to approximate NN weights that are used in cost function calculations. The resultant NN weights are:

W_L = [-8.4528 -0.0452 0.0018 92.5518 0.0001 0.1362 0.0000 0.0222]^T.

The proposed method can stabilize the after fault oscillations of the system's states effectively as shown in Fig. 4. It is also shown that when the weights are not approximated properly in the cost function, damping effect of the UPFC is deteriorated that results in more overshoot and settling time for the system states.

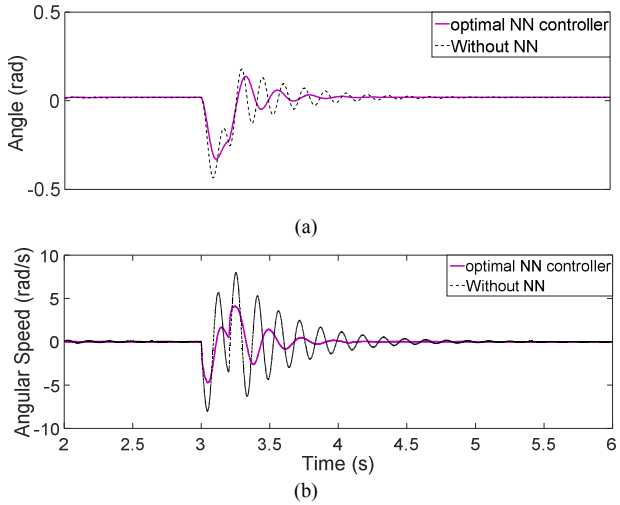

Fig. 4. Angle and angular speed of the synchronous generator-like DG unit equipped with UPFC with properly approximated weights and untuned weights

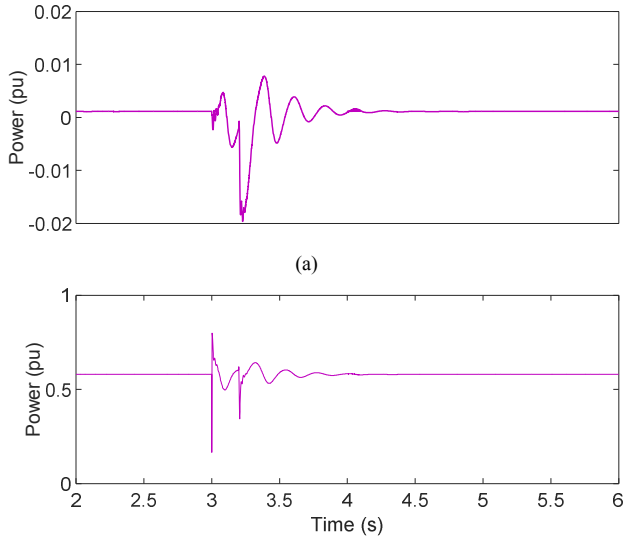

Fig. 5. Active power of transmision line and injected power of the UPFC

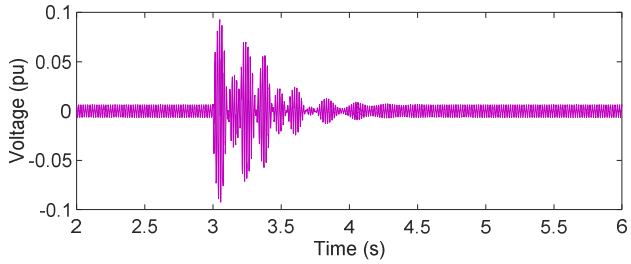

Fig. 6. Injected series voltage of the UPFC

The active power of the transmission line and also active power of the UPFC unit is depicted in Fig. 5. It is shown that the UPFC's active power is less than 2% of the nominal power. In addition, injected series voltage of the UPFC is less than 10% of the nominal voltage of the grid as demonstrated in Fig. 6.

Furthermore, an experimental setup is developed to test the theoretical analysis. The proposed modeling and control method is implemented using a dSPACE Microlabox control platform as shown in Fig. 7. The PV unit output voltage is delivered to a dc-dc buck converter. The buck converter provide a stable dc link voltage at the output. This dc voltage provide power for the three-phase inverter that feed the grid and also the inverter that generate series voltage of the UPFC unit. The LC filters are utilized to reduce voltage harmonics at the inverters output terminals. The output voltage of the main inverter feed a local load and the grid through a step up transformers. The output voltage of the UPFC inverter is also filtered, and then injected to the transmission line through the transformers that are positioned in series with the transmission lines.

Dc link voltage that is depicted in Fig. 8, shows voltage stability at the dc side. In addition, voltage of the grid at Bus 1 and also injected series voltage of the UPFC unit in normal condition of the microgrid is presented in Fig. 9 that displays stable operation of the entire system.

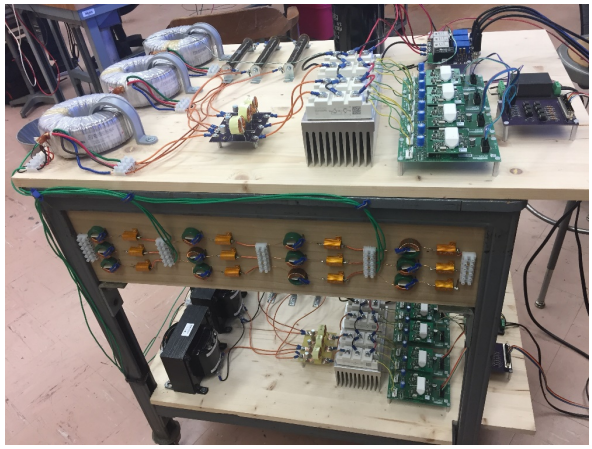

(a)

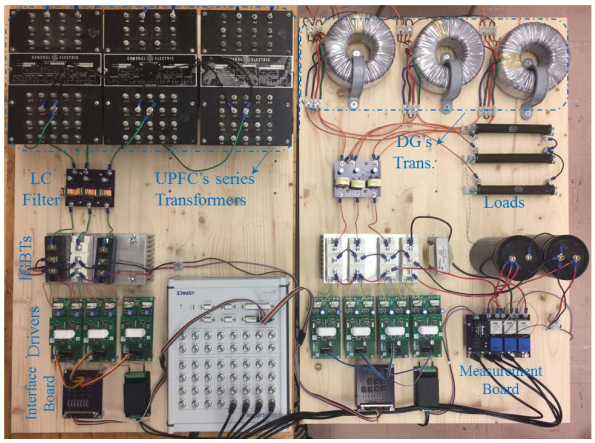

(b)

Fig. 7. The develpoed microgrid setup with two DG units and the DG+UPFC unit that is connected to the grid at Bus1 to enhance system stability

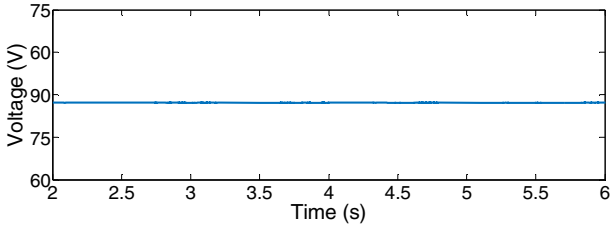

Fig. 8. Dc link voltage that feed both inverters of the DG+UPFC unit

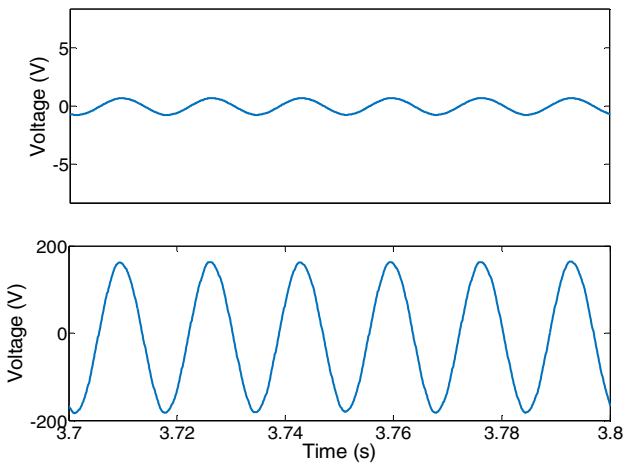

Fig. 9. Injected series voltage of the UPFC and grid voltage at Bus 1

V. CONCLUSION

A DG unit, composed of a PV source, dc-dc, and dc-ac converter, is modeled and controlled to behave like the classical model of a synchronous generator. Then, a novel reduced UPFC structure is presented and governed via an advanced optimal nonlinear control method to stabilize the DG unit in the micro grid environment. The proposed scheme could damp the system oscillations effectively. Although the proposed method is applied to the reduced UPFC structure in a micro grid environment, the scheme is applicable to traditional UPFCs in the power systems. The novel model is implemented for the first time and experiments are carried out that demonstrate the control scheme efficacy.

REFERENCES

[1] C. D. Schauder, L. Gyugyi, et al., "Operation of the Unified Power Flow Controller (UPFC) under Practical Constraints," IEEE Transactions on Power Delivery, vol. 13, no. 2, pp. 630-639, Apr. 1998.

[2] C. Li-Jun, and I. Erlich, "Simultaneous Coordinated Tuning of PSS and FACTS Damping Controllers in Large Power Systems," IEEE Transactions on Power Systems, vol. 20, no. 1, pp. 294 – 300, Feb. 2005.

[3] B. C. Pal, "Robust Damping of Interarea Oscillations with Unified Power-flow Controller," IEE Proceedings-Generation, Transmission, and Distribution, vol. 149, no. 6, pp. 733-738, Nov. 2002.

[4] N. Yang, Q. Liu., and J.D. McCalley, "TCSC Controller Design for Damping Interarea Oscillations," IEEE Transactions on Power Systems, vol. 13, no. 4, pp. 1304 – 1310, Nov. 1998.

[5] J. Guo, "Decentralized Control and Placement of Multiple Unified Power Flow Controllers," Missouri University of Science and Technology, PhD Dissertation, pp. 40-67, 2006.

[6] C.T. Chang, and Y. Y. Hsu, "Design of UPFC Controllers and Supplementary Damping Controller for Power Transmission Control and Stability Enhancement of a Longitudinal Power System," IEE proceedings, Generation, Transmission, and Distribution, vol. 149, no. 4, pp. 463-471, Jul. 2002.

[7] J. Guo, M. L. Crow, and J. Sarangapani, "An Improved UPFC Control for Oscillation Damping," IEEE Transactions on Power Systems, vol. 24, no. 1, pp. 288-296, Feb. 2009.J. Clerk Maxwell, A Treatise on Electricity and Magnetism, 3rd ed., vol. 2. Oxford: Clarendon, 1892, pp.68–73.

[8] Z. Chen and S. Jagannathan, "Generalized Hamilton–Jacobi–Bellman formulation-based neural network control of affine nonlinear discrete-time systems," *IEEE Trans. Neural Networks.*, vol. 10, no. 1, pp. 90–106, 2008

[9] F. L. Lewis and V. L. Syrmos, Optimal Control, 2nd ed. Hoboken, NJ: Wiley,1995.

[10] Nazaripouya, H., and S. Mehraeen. "Control of UPFC using Hamilton-Jacobi-Bellman formulation based neural network." Power and Energy Society General Meeting, 2012.

[11] H. Nazaripouya, and S. Mehraeen, "Modeling and Nonlinear Optimal Control of Weak/Islanded Grids Using FACTS Device in a Game Theoretic Approach," IEEE Transactions on Control Systems Technology, vol. 24, no. 1, pp. 158-171, Jan. 2016.

[12] S. M. Tayebi, C. Jourdan, and I. Batarseh, "Dynamic Dead Time Optimization and Phase-Skipping Control Techniques for Three-Phase Micro-Inverter Applications," IEEE Transactions on Industrial Electronics, vol. 63, no. 12, pp. 7523-7532, Dec. 2016.

[13] S. M. Tayebi, and I. Batarseh, "Analysis and Optimization of Variable-Frequency Soft-Switching Peak Current Mode Control Techniques for Microinverters," IEEE Transactions on Industrial electronics, vol. 33, no. 2, pp. 1644-1653, Feb. 2017.

[14] H. Saberi, and S. Mehraeen, "A Simultaneous Voltage and Frequency Control Scheme for Photovoltaic Distributed Generation Units in Small-scale Power Systems," Proc. Energy conversion Congress & Expo (ECCE), 2017.